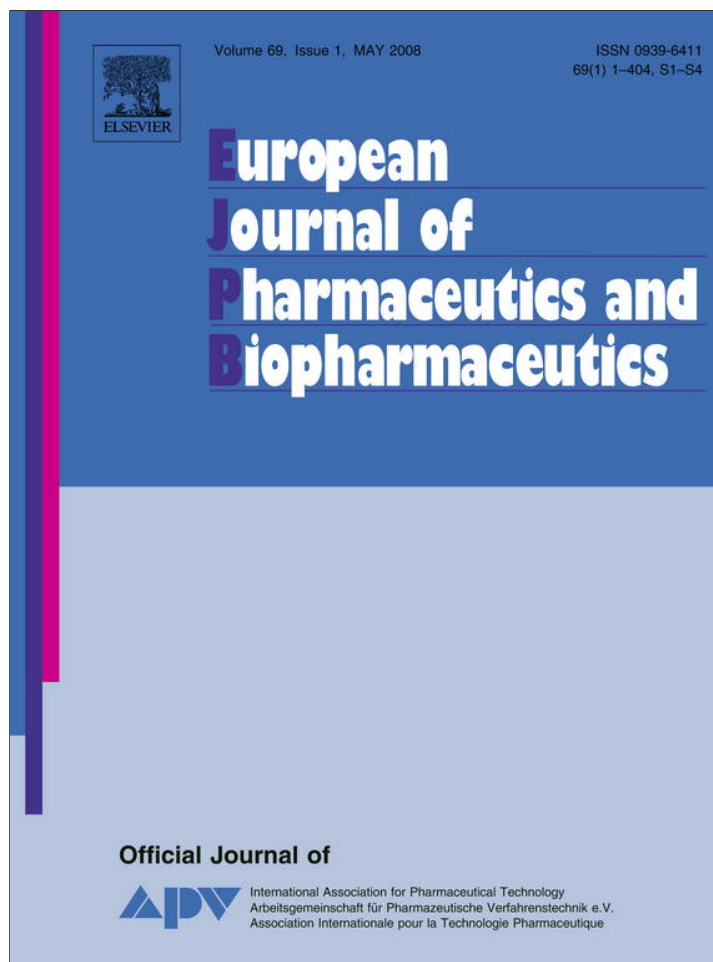


Provided for non-commercial research and education use.
Not for reproduction, distribution or commercial use.



This article appeared in a journal published by Elsevier. The attached copy is furnished to the author for internal non-commercial research and education use, including for instruction at the authors institution and sharing with colleagues.

Other uses, including reproduction and distribution, or selling or licensing copies, or posting to personal, institutional or third party websites are prohibited.

In most cases authors are permitted to post their version of the article (e.g. in Word or Tex form) to their personal website or institutional repository. Authors requiring further information regarding Elsevier's archiving and manuscript policies are encouraged to visit:

<http://www.elsevier.com/copyright>



ELSEVIER

Available online at www.sciencedirect.com

European Journal of Pharmaceutics and Biopharmaceutics 69 (2008) 106–116

**European
Journal of
Pharmaceutics and
Biopharmaceutics**www.elsevier.com/locate/ejpb

Research paper

Release pattern and structural integrity of lysozyme encapsulated in core–sheath structured poly(DL-lactide) ultrafine fibers prepared by emulsion electrospinning

Ye Yang, Xiaohong Li ^{*}, Mingbo Qi, Shaobing Zhou, Jie Weng*Key Laboratory of Advanced Technologies of Materials, Southwest Jiaotong University, Chengdu, PR China*

Received 8 July 2007; accepted in revised form 24 October 2007

Available online 4 November 2007

Abstract

The purpose of this study was to investigate the structural integrity, bioactivity and release patterns of lysozyme, as a model protein, encapsulated within the core–shell structured ultrafine fibers prepared by emulsion electrospinning. Electron microscopy and laser confocal scanning microscopy images demonstrated that the fibrous mats were very porous with integrally core–shell structured, bead-free, and randomly arrayed fibers. This structural property can pronouncedly alleviate the initial burst release and improve the sustainability of ultrafine fiber-based releasing devices. Sodium dodecyl sulfate–polyacrylamide gel electrophoresis and size exclusion chromatography were used to assess the primary structure of lysozyme, indicating that the ultra-sonication and electrospinning did not cause any remarkable denaturation of protein, while the core–shell structured fibers protected the structural integrity of encapsulated protein during incubation in the medium. Fourier transform infrared analyses showed that the electrospinning process had much less effect on the secondary structure of protein than ultra-sonication. The bioactivity assay indicated around 16% of specific activity loss during the emulsification procedure, and the protective effect of the shell materials on the activity of encapsulated protein. *In vitro* degradation showed that the protein entrapment led to more significant mass loss and higher molecular weight reduction.

© 2007 Elsevier B.V. All rights reserved.

Keywords: Emulsion electrospinning; Core–shell structure; Ultrafine fibers; Protein structures; Structural integrity; Bioactivity; *In vitro* release; Burst release

1. Introduction

Tissue engineering seeks to repair or replace damaged tissue using a combination of cell/molecular biology and material chemistry/engineering. There have been many attempts to make nano-featured scaffolds with controlled pore size, pore geometry, fiber dimension, and spatial orientation [1–3]. And all these features are essential for the transport of oxygen and nutrient supply to the cells and for the cellular growth, leading to tissue regeneration.

Biodegradable nanofibrous polymer scaffolds, prepared by an electrospinning technique, have a nanofibrous skeletal structure similar to that of extracellular matrix (ECM) present in the living tissue. The loosely bonding between fibers is beneficial for tissue ingrowth and cell migration and well distribution in the whole fibrous mats [4]. Besides these, with a three-dimensional open porous structure and high specific surface area, the nanofibrous polymeric scaffolds prepared by electrospinning technique can also deliver various bioactive agents in a sustained manner, such as antibiotics, anti-tumor agents, proteins, and plasmid DNA [5–8]. Li et al. studied silk fibroin fibers containing bone morphogenetic protein 2 (BMP-2) prepared via electrospinning as a bone tissue engineering scaffold. The results suggested that BMP-2 in the electrospun fiber led to higher calcium deposition and upregula-

^{*} Corresponding author. Key Laboratory of Advanced Technologies of Materials, Ministry of Education, School of Materials Science and Engineering, Southwest Jiaotong University, Chengdu 610031, PR China. Tel.: +86 28 87634023; fax: +86 28 87634649.

E-mail address: xhli@swjtu.edu.cn (X. Li).

tion of BMP-2 transcript levels when compared with the control group [9]. To maintain the structural stability and bioactivity of the encapsulated protein and to regulate the release profiles from the matrix fibers, while challenging, would greatly add to the probability for success of these materials.

The major disadvantages of the blend-electrospinning procedure are the severe burst release phenomenon and the reducing of effective lifetime of the device. Another problem is the influence of the processes of electrospinning, storage, and release on the structure and bioactivity of the incorporated proteins, which is crucial because of the complex physical and chemical instabilities inherent to protein. Salt-free dry lysozyme and polymer were dissolved into organic solvents, which was electrospun to produce lysozyme loaded fibrous meshes. A high initial burst (45%) with a low controlled release profile was detected, which attributed to the presence of untrapped lysozyme particles on the fiber surface [10]. Alternatively, it would be beneficial to address the raised issues by encapsulating or entrapping the drugs inside the nanofibers. The successful microencapsulation of protein within fibers could keep the stability and modulate the release behaviors of the entrapped substance. Recently, Qi et al. prepared Ca-alginate microspheres as a drug reservoir and dispersed the microspheres into a polymer solution. After electrospinning, fibers with beads-on-string structures were obtained. Compared with the uncoated Ca-alginate microspheres, prolonged release profiles and lower burst release were achieved, but there were 50–70% of the encapsulated protein released out during the initial 20 h [11]. In recent years, a coaxial dual-capillary spinneret has been employed in electrospinning to fabricate core–sheath nanofibers [12,13]. Zhang et al. investigated the feasibility of encapsulated bovine serum albumin (BSA), along with poly(ethylene glycol), into biodegradable poly(ϵ -caprolactone) nanofibers via the coaxial electrospinning technique. It was found that the initial burst release, which occurred over a period of 2 days, accounted for 45–65% of protein from the core–sheath structured fibers versus 60–70% from blended fibers [12]. It was also noted that the equipment design and electrohydrodynamic behaviors of the coaxial electrospinning were complex, and that the selection of the solvent for the inner solution and the control of the spinning parameters had a dramatic influence on the structure of the fibers, especially when a water-soluble polymer was incorporated within the inner core.

Emulsion electrospinning was a novel process to prepare core–sheath fibers. It had been successfully applied to the encapsulation of poly(ethylene oxide) and doxorubicin hydrochloride in the shell material of poly(ethylene glycol)-poly(L-lactic acid) [14,15]. Until now, the stability and release profile of proteins, which can also be spun into the inner core, have not been investigated. In the current study, emulsion electrospinning was introduced to prepare core-shell structured composite fibers (lyz-MC/PDLLA) with the lysozyme, as the model protein, encapsulated into

the poly (DL-lactic acid) (PDLLA) fibers along with methyl cellulose (MC). Lysozyme was chosen as the model protein as its similar size with most growth factors and many well investigated aspects, including stability and structure. Lysozyme in phosphate buffer saline (PBS) was emulsified into PDLLA solution under ultra-sonication, and the emulsion was electrospun by ordinary equipment. The fiber characteristics, protein release profile, structural integrity, bioactivity and matrix polymer degradation were investigated in detail.

2. Materials and methods

2.1. Materials

PDLLA with molecular weight of 54 kDa was synthesized in our laboratory [16]. The molecular weight was determined by gel permeation chromatography (GPC, Waters 2695 and 2414, Milford, MA) with a Styragel HT 4 column (7.8 × 300 mm) using polystyrene beads as standard. Tetrahydrofuran (THF) was used as the mobile phase at a flow rate of 1.0 ml/min. Lysozyme (EC 3.2.1.17, Mw: 14.4 kDa, 6800 IU/mg) and FITC were purchased from Sigma–Aldrich Inc. (St. Louis, MO). MC (300–500 mPa s) was obtained from Chengdu Kelong Reagent Co. (Chengdu, China). SDS–PAGE molecular weight marker for protein was purchased from Institute of Biochemistry, Chinese Academy of Sciences (Shanghai, China). *Micrococcus lysodeikticus* dried cells were supplied by China Center for Type Culture Collection (Wuhan, China). Ultra-pure water from a Milli-Q biocel purification system (UPI-IV-20, Shanghai UP Scientific Instrument Co., Ltd, Shanghai, China) was used in all experiments. All other chemicals and solvents were of reagent grade or better.

2.2. Electrospinning

Lysozyme was dissolved in PBS (50 mM, pH7.4) with MC and the solution was dropped into the PDLLA chloroform solution, followed by ultra-sonication in an ice bath (VC 505, Sonics & Materials, Inc., Newtown, CT). Emulsions E1, E2, and E3 were prepared with the following ratios of protein to polymer: 1.0%, 3.0%, and 5.0% (w/w), respectively. The resulting fibers (lyz-MC/PDLLA) F1, F2, and F3 were obtained by electrospinning through previously described equipment to provide the composite fibers on the collector as described elsewhere [17]. Briefly, the emulsion was added in a 5-ml syringe attached to a metal capillary with the exit orifice diameter of 0.6 mm. The electrospinning apparatus was equipped with a high-voltage statitron (Tianjing High Voltage Power Supply Co., Tianjing, China), and the flow rate of the drug–polymer solution was controlled by a microinject pump (Zhejiang University Medical Instrument Co., Hangzhou, China). The control samples of fiber without lysozyme entrapment but with MC (MC/PDLLA) were also pre-

pared as described above. In order to visualize the protein distribution in electrospun fibers, lysozyme was labeled with FITC, which emitted a green fluorescence. FITC was reacted with an aqueous solution of lysozyme in the dark under stirring for 24 h at 4 °C. The reaction mixture was dialyzed to remove any residual FITC and freeze-dried. The labeled fibers (fitc-lyz-MC/PDLLA) were obtained by electrospinning labeled protein (fitc-lyz) along with MC as mentioned above. All the fibrous mats were lyophilized overnight to remove any solvent and water residues and stored at 4 °C in a desiccator for further use.

2.3. Fiber characterization

The electrospun nanofibrous mats, mounted on metal stubs by using conductive double-sided tape, were sputter-coated with gold for a period up to 120 s. Their morphologies were then observed by scanning electron microscope (SEM, Quanta 200, FEI, Netherlands) at an accelerating voltage of 20 kV. The fiber diameter was measured from SEM images, and five images were used for each fiber sample. From each image, at least 20 different fibers and 100 different segments were randomly selected and their diameters were measured to generate an average by using Photoshop 8.0 edition. The core-sheath structure of the electrospun lyz-MC/PDLLA composite ultrafine fibers was examined with laser confocal scanning microscope (LCSM, Leica TCS SP2, Germany) and transmission electron microscope (TEM, HITACHI H-700H, Japan). When the composite ultrafine fibers were observed under LCSM, electrospun MC/PDLLA fibers were used as the negative control. Excitation and emission wavelengths were 488 and 535 nm, respectively. In brief, all the parameters including the laser intensity and gain were adjusted until fluorescent signals could not be seen from the control sample; then without changing the settings, the same parameters were used to observe fiber samples based on fitc-lyz-MC/PDLLA. TEM was operated at 15 kV, and the fiber samples were prepared by directly depositing the as-spun ultrafine fibers onto copper grids.

2.4. Characterization of encapsulated protein within fibers

Core loading of lysozyme in the ultrafine fibers was determined by extracting the protein content from fibers. In brief, a known amount of fibers (ca. 100 mg) were dissolved in chloroform (500 μ L) and extracted three times with double-distilled water (600 μ L). The lysozyme content of the extracted solution was determined by UV-vis spectrophotometer (UV-2550, Shimadzu, Japan) based on the method of Bradford [18], in which the concentration was obtained using a standard curve from known concentrations of lysozyme solutions. The extraction efficiency was calibrated by adding a certain amount of lysozyme and MC solution into PDLLA/ CHCl_3 solution along with the same concentration as above and extracted using the

above-mentioned process. The analysis of lysozyme located at the fibers surface based on the displacement of surface-adsorbed protein by sodium dodecyl sulfate (SDS), a powerful negatively charged detergent, which could bind to the hydrophobic regions of protein molecules causing them to unfold into extended polypeptide chains and freeing them from their associations with other molecules [19]. Briefly, ultrafine fibers (5–7 mg) were accurately weighed and suspended in SDS solution (2 ml, 2%, w/v) and agitated for 4 h at room temperature. The samples were centrifuged and the supernatant was analyzed for protein. And the surface protein content indicated the percentage of the amount of lysozyme at surface with respect to the total amount encapsulated within the fibers. The lysozyme content was determined in triplicate for at least three different batches.

2.5. Determination of the primary structure of lysozyme

To detect the aggregation and degradation of lysozyme molecules during the fiber preparation and release period, the lysozyme was extracted from the obtained emulsions and electrospun fibers. The emulsions were destabilized by the addition of excess buffer, followed by centrifugation (Anke TGL-16B, Shanghai Anting Scientific Instrument Co., Ltd, Shanghai, China) at 4000g for 5 min. The lysozyme extraction from electrospun fibers were performed by dissolving a known amount of fiber mat in methylene chloride followed by extracting three times with PBS. The extractants were assessed by Sodium dodecyl sulfate–polyacrylamide gel electrophoresis (SDS–PAGE), and high performance liquid chromatography (HPLC, Waters 2695, Milford, MA) with an Ultrahydrogel 250 column (7.8 \times 300 mm, Waters, Milford, MA). The mobile phase was pH 7.4, 50 mM phosphate buffer containing 0.3 M sodium chloride with the flow rate of 0.5 ml/min. Polyethylene glycols were also run under identical chromatographic conditions to serve as molecular weight standards. Triplicate measurements were made for each sample, and the chromatograms were processed using Empower software (Waters, Milford, MA). To evaluate the effect of extraction process on the molecular structure, free fresh lysozyme was added in MC/PDLLA, which was dissolved in methylene chloride, then extracted by PBS under the same conditions as above.

2.6. Determination of the secondary structure of lysozyme

Fourier transform infrared (FTIR) was used for the analysis of the secondary structure of lysozyme [20], and were recorded using a Nicolet 5700 FTIR spectrometer (Madison, WI). Samples were centrifuged at 4000g at 4 °C to precipitate possible impurities and placed in CaF_2 windows with 20 μ m path length. Fourier self-deconvolution was performed with software Omnic 7.2, and the deconvoluted spectra were fitted using Gaussian band profiles using the software OriginPro 7.5. To measure the over-

all perturbations in the protein structure, spectral correlation coefficients were calculated between the Amide I second derivative spectrum of free fresh lysozyme in aqueous solution and those at various stages of processing as described by Perez et al. [21]. The spectral correlation coefficient was calculated using software Matrix Laboratory 7.0, and identical spectra (and thus structures) resulted in a value of 1.0. Furthermore, the assignment of the individual secondary structural elements from the derivative and the deconvoluted Amide I region was carried out according to Karen Fu et al. [22]. Integration of each Gaussian provided the relative content of the respective secondary structure. The secondary structure contents were calculated from the areas of the individual assigned bands and their fraction to the total area in the Amide I region for at least three spectra. All samples were measured at least six times.

2.7. Lysozyme activity assay

Lysozyme is effective to digest Gram-positive cell walls and hence the rate of lysis of *M. lysodeikticus* cells was used to estimate the bioactivity of the enzyme as described by Meng et al. [23]. Briefly, 150 μL of the lysozyme samples or standards (0–25 mg/ml) were added to a 96-well microplate. A suspension of *M. lysodeikticus* cells (100 μL , 2–3 mg/ml) was added, and the turbidity at 450 nm was measured by μQuant microplate spectrophotometer (Elx-800, Bio-Tek Instrument Inc., Winooski, VT) at 15 s intervals for 4 min at 37 °C. The lysozyme activity for the corresponding initial rate of a sample was calculated from a standard curve of the log concentration vs. initial rate. Results were expressed as the initial kinetic rate (slope of the OD vs. time at $t = 0$), assuming that one unit of enzyme activity was equivalent to an absorbance decrease of 0.001 absorbance unit per minute. Specific activity was defined in terms of units of activity per milligram of protein (U/mg). All samples were assayed in triplicate.

2.8. In vitro protein release

The fibrous lyz-MC/PDLLA mat was first punched into small squares ($2 \times 2 \text{ cm}^2$) with a total mass of ca. 200 mg, which were immersed in 10 ml of PBS (pH7.4) containing 0.02% sodium azide as a bacteriostatic agent. The suspension was kept in a thermostated shaking water bath (Tai-chang Medical Apparatus Co., Jiangsu, China) that was maintained at 37 °C and 100 cycles/min. At predetermined time intervals, 1.0 ml of the release buffer was removed for analysis and 1.0 ml of fresh PBS was added back for continuing incubation. The lysozyme amount present in the release buffer was determined as described above. The MC/PDLLA fibers with the addition of the same amount of lysozyme as that in the lyz-MC/PDLLA fibers were used as a control for protein determination. Triplicate composite fiber mats were analyzed in each trial.

2.9. In vitro matrix degradation

To check the effect of protein incubation on the degradation profiles of electrospun fibers, lyz-MC/PDLLA, and MC/PDLLA fibrous mats were accurately pre-weighed (ca. 100 mg each) and added to 5.0 ml of PBS (pH 7.4), containing 0.02% sodium azide as a bacteriostatic agent. At predetermined time intervals, a group of each was retrieved, rinsed with distilled water to remove residual buffer salts, and dried to constant weight in a vacuum desiccator. The mass loss was determined gravimetrically by comparing the dry weight remaining at a specific time with the initial weight. The molecular weight of recovered matrix polymer was determined by GPC using the same method as mentioned above. The morphology of the samples was observed with SEM as described previously. All samples were assayed in triplicate.

2.10. Statistics analysis

Values were expressed as means \pm standard deviation (SD). Statistical significance of differences was examined using one-way analysis of variance (ANOVA) followed by LSD post hoc test. A probability value (p) of less than 0.05 was considered to be statistically significant.

3. Results and discussion

3.1. Fiber characterization

Fig. 1 shows the fibrous morphology and inner structures of the lyz-MC/PDLLA fibers prepared by emulsion electrospinning. SEM images (Fig. 1a–c) illustrated that fibrous mats were porous with bead-free and randomly arrayed fibers. Lysozyme is a water-soluble, globular protein and non-electrospinnable, per se, in this study, it had little influence on the formation of fibrous structure. The diameters of fiber samples F1, F2, and F3 were 620 ± 200 , 580 ± 180 , and 570 ± 110 nm prepared from emulsions with weight ratios of proteins to matrix polymers of 1.0%, 3.0% and 5.0% (w/w), respectively. Statistical analysis showed that there was no significant difference ($p > 0.05$) on the fiber diameters, due to the same continuous phase of the emulsion used in the three groups.

As the SEM images cannot provide evidences that lysozyme was successfully encapsulated inside the fibers, several means to characterize the encapsulation profiles were employed. First, lysozyme was labeled with FITC, and the composite fibers (fitc-lyz-MC/PDLLA) were observed under LCSM. Fig. 1d showed that the fibers emitted green light, suggesting the presence of the labeled lysozyme. Fig. 1e gives a representation of the same fiber with and without excitation superimposed on one another showing that the composite fibers prepared by emulsion electrospinning contained a core–sheath structure. TEM was also applied to obtain further evidence that lysozyme was indeed encapsulated within the shell material (Fig. 1f). It

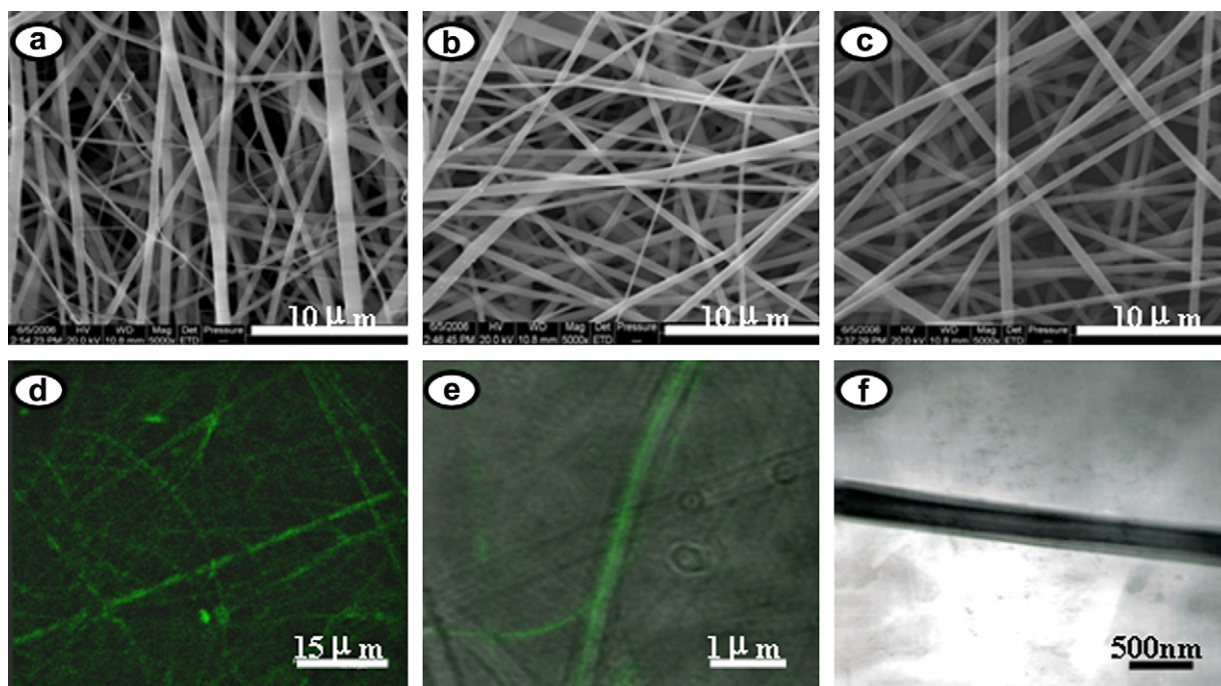


Fig. 1. Fiber morphologies and inner structures of lyz-MC/PDLLA composite fibers. SEM images of fiber samples F1, F2 and F3 prepared from emulsions with weight ratios of proteins to polymers of 1.0% (a), 3.0% (b) and 5.0% (c). Overview LCSM image of fiber sample F1 (d); LCSM (e) and TEM images (f) of a segment of fiber sample F1.

can be seen that the lysozyme was wrapped into the center of the composite fibers of lyz-MC/PDLLA. The sharp boundaries in the TEM images were indicative of the difference of electron transmission ability between the core and shell materials. The likely reasons for these areas of sharp contrast may be associated with the immiscibility of the aqueous and organic phases and the very fast processing characteristic of electrospinning, which would prevent the two fluids from mixing significantly [24].

Coaxial electrospinning has been used to prepare ultra-fine fibers with core–sheath structures, in which two components can be coaxially and simultaneously electrospun through different feeding capillary channels to generate composite nanofibers. It has been noted that only part of the obtained fibers exhibited a core–shell structure [12]. One possible reason for this was that the two components were mixed only at the exit orifice of injection needles. The coaxial electrospinning was a dynamic process, and factors such as flow rate of the inner and outer fluids, interfacial tension, and viscoelasticity of the two polymer fluids could affect entrainment and produce fibers without the required core–sheath morphology [13]. Therefore, in the coaxial electrospinning process, a special apparatus and careful selection of operational parameters were needed to ensure the desired results. In the emulsion electrospinning process, which was used in current study, the emulsion droplets moved perpendicularly from the surface to the center so as to achieve their enrichment in the axial region, which were stretched into an elliptical shape in the direction of the fiber trajectory. This inward movement of emulsion droplets was caused by rapid elongation and evaporation

of the solvents during electrospinning. As chloroform evaporated faster than water, the viscosity of the outer layer of the fiber increased more rapidly than that of the inner layer. It is this viscosity difference between the elliptical droplets and the polymer matrix that directed core materials to settle into the fiber interior rather than on the surfaces [11]. But in the sample F3, there were also cases of irregular movement of the inner component with an obvious oblique portion very close to the fiber surface as illustrated by TEM segment (data not shown). A possible reason was that excess addition of protein into the emulsion droplets led to a higher outward diffusion of proteins into the polymer solution during electrospinning process. This would likely affect the protein distribution within fibers, the release profiles, and the structural stability and bioactivity of encapsulated proteins during incubation.

3.2. Characterization of encapsulated lysozyme in fibers

Loading amounts of lysozyme were close to the theoretic values for all the fiber samples, and the surface protein content of samples F1, F2, and F3 were $11.2 \pm 0.4\%$, $15.4 \pm 0.4\%$ and $24.2 \pm 0.5\%$, respectively. The larger distribution of proteins on the fiber surface should be resulted from the higher outward diffusion of proteins into the polymer solution during electrospinning process. In order to develop a successful protein delivery system, it is essential that the biological activity should be retained throughout the fiber preparation process and incubation into the release medium. The primary and secondary structures, the specific activity retention were detected with regard to

the initial protein loadings, the ultra-sonication and electrospinning process.

The influence of ultra-sonication and electrospinning on the structure of lysozyme was assessed with SDS–PAGE by comparing the data with that of native lysozyme and molecular weight standards. As shown in Fig. 2A, it can be seen that no remarkable structural changes occurred in the proteins during ultra-sonication and electrospinning as no aggregation or hydrolysis was detected in the gel. Due to the low sensitivity of SDS–PAGE, HPLC was also used to investigate the structural integrity of lysozyme under different conditions. As shown in Fig. 2B-a, native lysozyme showed a major peak at ca. 14.4 kDa, which corresponded to the monomeric protein. After the processing by ultra-sonication (Fig. 2B-b) and electrospinning (Fig. 2B-c), the chromatograms of extracted lysozyme had not shown remarkable aggregation or degradation, and it was almost identical with the native lysozyme. Same HPLC profiles were detected for emulsion samples E2 and E3 and fiber samples F2 and F3.

FTIR is an established technique for the analysis of the secondary structure of proteins in solution [25]. Typically, the Amide I band (mainly C=O stretching mode of the protein backbone) appears at 1656 cm^{-1} with a shoulder

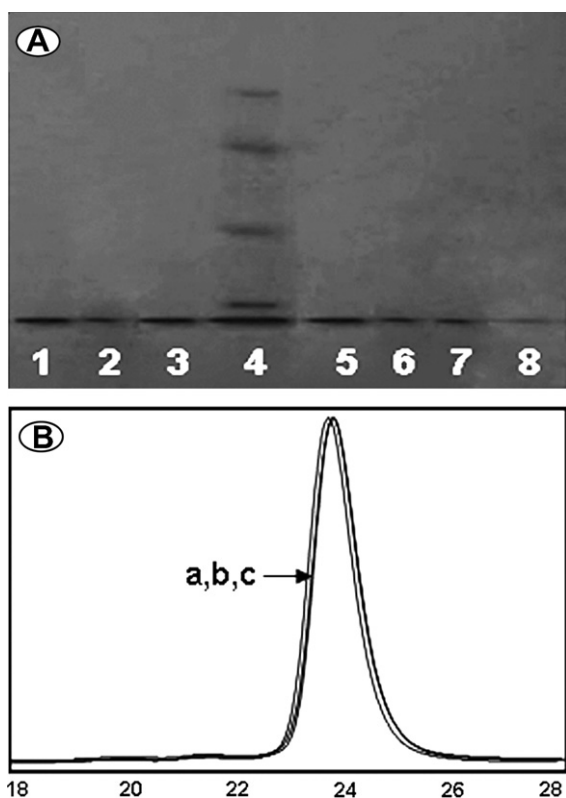


Fig. 2. (A) SDS–PAGE of lysozyme: lanes 1–3, extracted from emulsion samples E1, E2, and E3 with weight ratios of proteins to matrix polymers of 1.0%, 3.0% and 5.0%; lane 8, 7 and 6, extracted from fiber samples F1, F2, and F3 after electrospinning emulsions E1, E2 and E3; lane 4: MW standard ladder; lane 5: native lysozyme; (B) HPLC peaks of native lysozyme in 50 mM, pH 7.4 PBS (a), extracted from emulsion sample E1 (b) and fiber sample F1 (c).

at 1628 cm^{-1} . The former frequency confirms the existence of different secondary structures of the protein backbone [26]. It is well known that the individual bands contained in the deconvolved Amide I contour can be assigned to particular types of protein secondary structure. The qualitative assignment of the overlapping components of the Amide I band to secondary structure is based upon a comparison with the spectra of proteins of known structure based on X-ray crystallography. According to the widely accepted assignment for the characteristic absorptions of Amide I region of lysozyme, the β -sheet primarily vibrate around 1630 cm^{-1} , α -helix around 1655 cm^{-1} , and β -corners from around 1663 to 1700 cm^{-1} [27]. Areas of different components of the deconvolved spectrum can be associated with the ratios of different types of secondary structure [28]. Fig. 3 shows the Amide I region of FTIR spectra of native lysozyme (Fig. 3a) and the Gaussian fitting curves

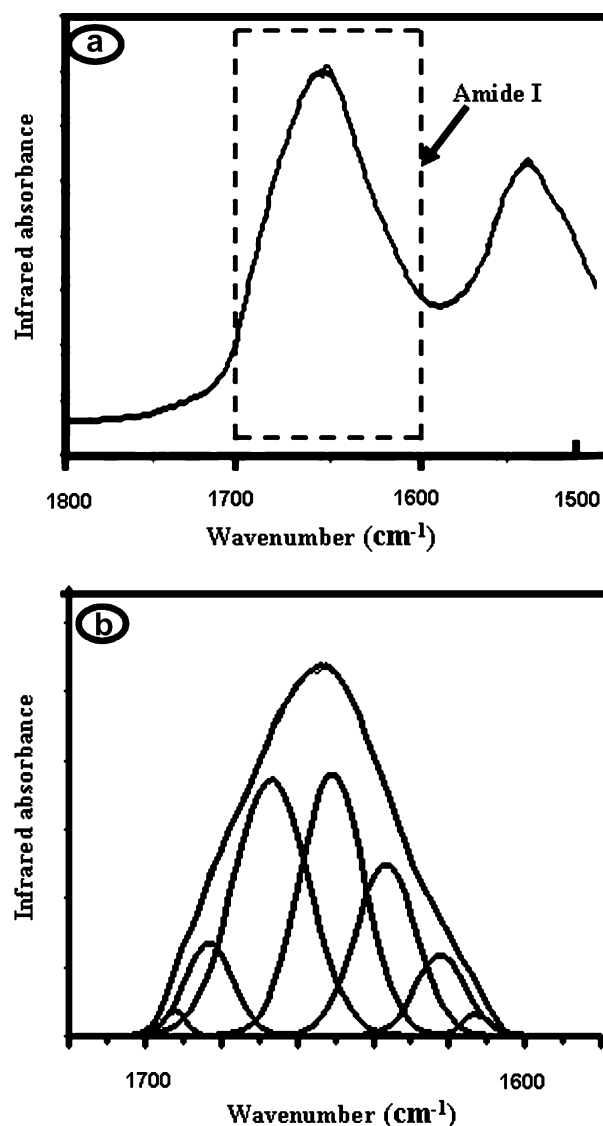


Fig. 3. Amide I region (a) and Gaussian curve-fitting Amide I region (b) of FTIR spectrum of native lysozyme in 50 mM, pH 7.4 PBS.

(Fig. 3b). Analysis of the Amide I region of lysozyme revealed the secondary structure to be $34.1 \pm 2.5\%$ of α -helix (1651.0 cm^{-1}), $29.2 \pm 1.7\%$ of β -sheet (1616.7 and 1630.6 cm^{-1}), and $36.6 \pm 2.9\%$ of β -corner (1662.9 , 1672.1 , 1682.2 and 1691.8 cm^{-1}), as determined by Gaussian curve-fitting. This result was in agreement with previous FTIR studies of lysozyme [29]. Generally, protein/peptide aggregation involved mostly β -sheet while α -helix structures seemed to be less likely to form aggregates. This may be due to a stronger dipole moment of α -helices than that of β -sheets [30]. So in our study, the β -sheet content was to be an indicator of the protein structural integrity.

Lysozyme extracted from the emulsions and electrospun fibers were tested as mentioned above. Some controls were run to ensure that the results were not an artifact of the sample preparation technique. The matrix PDLLA and the additive MC showed no effect on the Amide I area of the FTIR spectrum of lysozyme. Lysozyme was extracted from mixture of electrospun MC/PDLLA fibers and the fresh lysozyme, and showed that the extraction process had no influence on the Amide I region of the secondary structure of lysozyme. Table 1 summarizes the overall spectral correlation coefficients of the Amide I second derivative spectrum and the contents of subcomponents of secondary structure determined by Gaussian curve-fitting of the FTIR spectra of lysozyme under different processing conditions. In general, the process of ultra-sonication and electrospinning did not cause any remarkable changes of the spectral correlation coefficients. And the increase in the protein loading amounts led to small increase in the β -sheet content. It indicated a slight aggregation of the lysozyme occurred in the composite fibers with higher protein inoculation due to the inefficient encapsulation of protein within the fibers.

As indicated in Table 1, about 16% of specific activity loss was detected after the emulsification procedure, independent on the protein loadings. There was significant activity loss ($p < 0.05$) for all the emulsion samples compared with the native protein. The electrospinning process led to much less activity loss, and there was no significant difference in the specific activity retention between the emulsification and electrospinning process ($p > 0.05$). The emulsification and ultra-sonication procedures, in which

lysozyme exposed to matrix polymer and organic solvents, would dissipate the protein hydrophobic cores in contact with the solvent and disrupt the protein hydration shell, leading to destabilization and unfolding of protein. Through the analysis of the primary and secondary structures and the specific activity retention, it suggested that the best way to prevent denaturation and activity loss of protein was to optimize the emulsion components and emulsification procedures to minimize their exposure to the matrix polymer, organic solvents and dispersion forces.

3.3. *In vitro* protein release

Fig. 4 shows the lysozyme release profiles from the core-sheath structured composite fibers. The release kinetics for all the fibers with different amounts of lysozyme entrapment can be illustrated in two stages: an initial fast release followed by a constant linear release. The burst releases from fibers samples F1, F2, and F3 accounted for $26.8 \pm 1.5\%$, $41.1 \pm 1.8\%$ and $47.1 \pm 4.5\%$ in initial 12 h, respectively. Statistical analysis indicated that there were significant differences among these groups ($p < 0.05$). As indicated above,

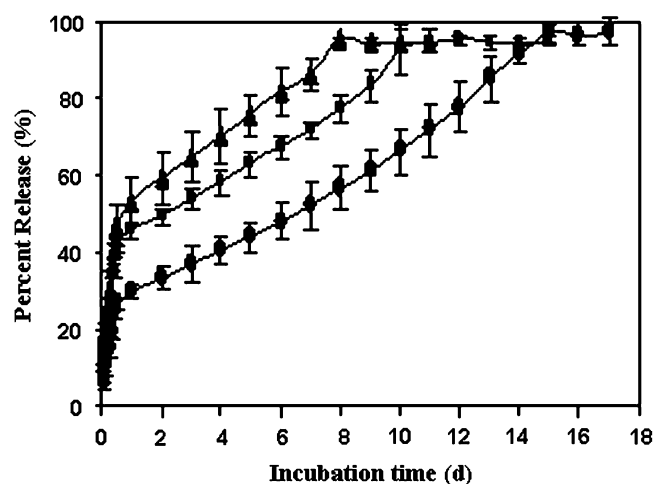


Fig. 4. *In vitro* release profiles of lysozyme from fiber samples F1, F2 and F3 with protein loadings of 1.0% (●), 3.0% (■) and 5.0% (▲) ($n = 3$).

Table 1

The spectral correlation coefficient and the contents of subcomponents of secondary structures of the Amide I region of FTIR spectra, and the specific activity retention of lysozyme under various conditions

Lysozyme samples	Secondary structure content (%)			Spectral correlation coefficient	Specific activity retention (%)
	α -Helix	β -Sheet	β -Corner		
Native	34.1 ± 2.5	29.2 ± 1.7	36.6 ± 2.9	1.000	100
Extracted from E1 ^a	33.9 ± 1.1	30.5 ± 1.0	35.6 ± 1.5	0.999 ± 0.001	84.6 ± 2.7
Extracted from E2 ^a	32.5 ± 2.1	32.3 ± 1.4	35.1 ± 1.7	0.997 ± 0.003	83.8 ± 3.3
Extracted from E3 ^a	30.6 ± 3.9	34.7 ± 2.2	35.7 ± 3.6	0.996 ± 0.004	84.4 ± 2.2
Extracted from F1 ^b	33.6 ± 1.1	30.6 ± 0.8	35.8 ± 2.0	0.998 ± 0.002	83.3 ± 3.2
Extracted from F2 ^b	32.3 ± 1.8	33.3 ± 2.2	33.9 ± 1.1	0.996 ± 0.001	82.5 ± 2.1
Extracted from F3 ^b	30.0 ± 2.9	34.0 ± 2.2	35.9 ± 3.0	0.996 ± 0.003	83.9 ± 3.1

^a E1, E2 and E3 were emulsions with weight ratios of protein to polymer of 1.0%, 3.0% and 5.0%, respectively.

^b F1, F2, and F3 were fibers prepared from emulsions E1, E2 and E3, respectively.

emulsions with higher protein loadings led to fibers with less integrity of the core–shell structure, resulting from a higher outward diffusion of proteins into the polymer solution during electrospinning process. The core materials of lysozyme would initially diffuse out through the imperfections of core–sheath structure, such as very thin shell to favor good permeability and the shell failure.

As shown in Fig. 4, after this initial burst release, the core–sheath composite fibers with different amounts of lysozyme inoculation released proteins at a constant rate for several days, which may be attributed to the diffusion of the protein from the cores through the fibers or aqueous pores therein. However, sustainability of lysozyme release from the various composite fibers was different. It can be seen that the increase of lysozyme loading led to a reduction in the effective lifetime of the releasing device, which may be due to the thinner shell phase and more porous shell matrix for agents to release faster from the device. And inclusion of the relatively large amount of water soluble proteins in the core–sheath device would potentially give rise to an osmotic effect to pump the inner agents out as the shell matrices were hydrated and water molecules penetrated into the core, causing dilution and swelling of the inner components to diffuse out rapidly.

Our current study indicated that core–sheath structure can apparently alleviate the initial burst release and provide a constant rate of release over a significant portion of the lifetime of the device. This conclusion was also in agreement with results obtained from other similar core–shell-type configurations such as microspheres [31] and fibers [12]. However, reservoir release rates were also found to be critically dependent on the integrity of core–shell structures, shell thickness, surface area and permeability. Qi et al. encapsulated protein-loaded Ca-alginate microspheres into polymer fibers generating beads-on-string morphologies. The polymer shells around the beads were too thin to modulate protein release, and over 40% of proteins were released from the fibers during the initial 12 h [11]. Zhang et al. encapsulated BSA into poly(ϵ -caprolactone) via the coaxial electrospinning with the result that only a part of the obtained fibers exhibited core–shell structure. *In vitro* release studies showed that over 50% of the protein release was observed for fibers with only 0.2% of BSA entrapment [12]. In the current investigation, more well-defined core–shell structures were observed for fibers prepared by the emulsion electrospinning process, and around 27% of the burst release was detected from fibers with a 1.0% of lysozyme loading, followed by sustained releasing for 2 weeks. Furthermore, 1% of protein loading should be high enough such that ultrafine fibers might be applicable to the delivery of growth factors as tissue engineering scaffold.

3.4. Structural integrity and bioactivity of lysozyme during *in vitro* release

It indicated that the degradation of the matrix polymers during incubation in the medium had some effects on the

Amide I area of FITR spectrum of lysozyme. And the secondary structures of proteins in the medium and within the fiber matrix during *in vitro* release period have not been determined. Fig. 5A–C show the HPLC peaks of encapsulated lysozyme after incubating the electrospun lyz-MC/PDLLA fibers in PBS (50 mM, pH 7.4) for 1 day, 1 week and 2 weeks, respectively. Compared with the native protein (Fig. 5a), it can be seen that the major peak shifted to lower molecular weights, which corresponded to the degradation of lysozyme (Fig. 5b–d). Except fiber sample F1 after incubation for 1 day, other peaks at higher molecular weight region appeared, indicating the aggregation of lysozyme. Because of the longer exposition to the medium, the aggregation degrees, which were related with the area ratios of the high molecular weight peaks to the lower ones, increased with the incubation time from 1 day (Fig. 5b) to 2 weeks (Fig. 5d). Compared with the encapsulated lysozyme, a much higher aggregation degree and larger shift of major peak to lower molecular weight were detected (Fig. 5e) from the free lysozyme incubated with MC/PDLLA fibers, indicating that the core–shell-structured electrospun fibers could protect the structural integrity of encapsulated lysozyme during incubation in the medium. And a decrease in the observed protective effect was demonstrated for fibers prepared from primary emulsions with increased weight ratios of protein to polymer from 1.0% to 5.0% (Fig. 5A–C). This maybe attributed to the poorly formed core–shell structure for fibers prepared from higher protein loadings as described above.

The retention of specific bioactivity was evaluated for lysozyme entrapped within electrospun fibers during incubation in the *in vitro* release medium. The bioactivity loss may be attributable to possible interactions between lysozyme and the incubation medium and the degradation products of matrix polymers. As shown in Fig. 5D, the specific activity retention was significantly higher for lysozyme encapsulated within lyz-MC/PDLLA fibers than free lysozyme incubated with MC/PDLLA fibers ($p < 0.05$). This was due to the protective effect of core-shell-structured fibers. There was significant higher loss of specific activity for fibers with higher protein loadings ($p < 0.05$ for all pair-wise comparisons), due to the insufficient protective effect of the polymer shell to the core materials for high protein entrapment.

3.5. *In vitro* matrix degradation

A biodegradable polymer-based scaffold must be able to support attachment, proliferation and differentiation of cells, as well as maintaining suitable mechanical properties until tissues is regenerated at the injured site. To evaluate the effect of protein incorporation on the degradation profiles of electrospun fibers, the mass loss, molecular weight reduction and morphology changes were detected for matrix residues of lyz-MC/PDLLA and MC/PDLLA fibrous mats. Fig. 6 shows the morphologies of fibers after 2 (Fig. 6a), 4 (Fig. 6b) and 8 (Fig. 6c) weeks of incubation.

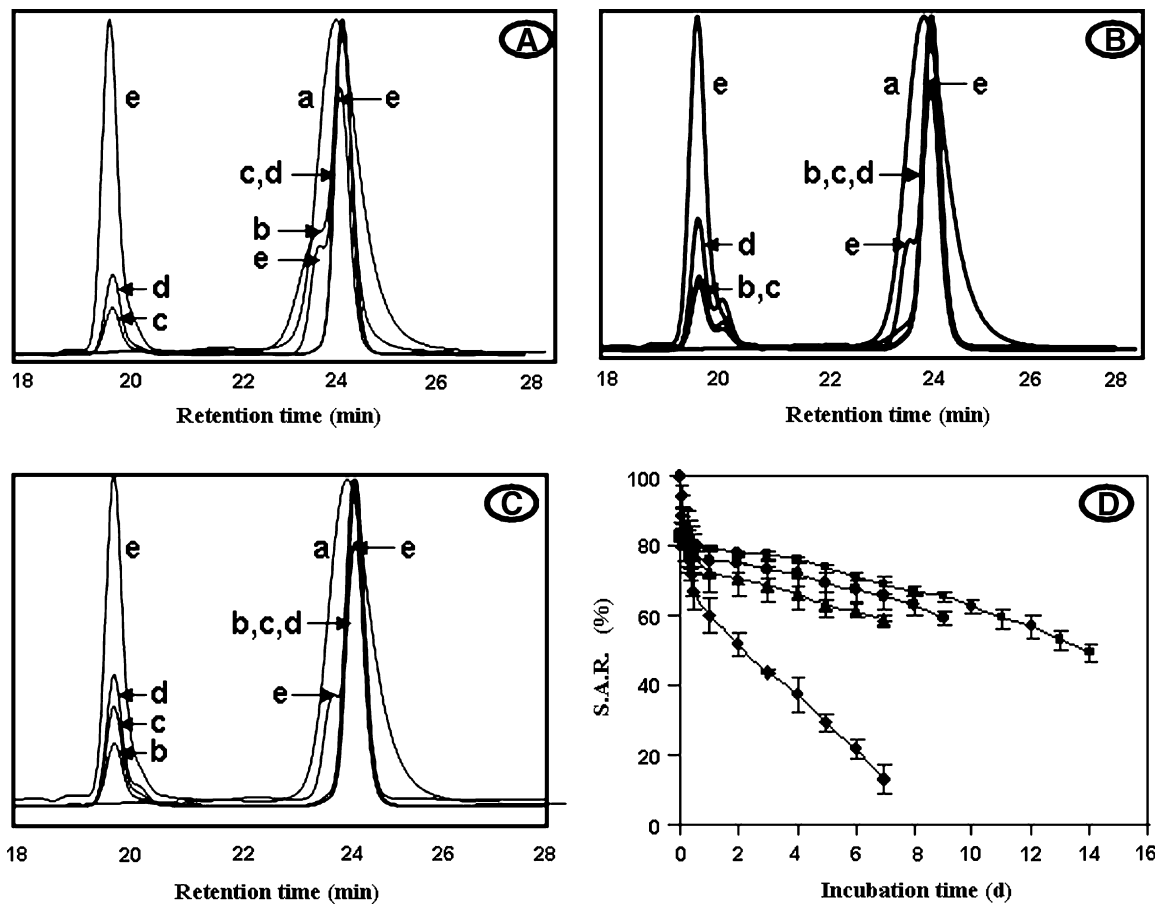


Fig. 5. (A–C) HPLC peaks of native lysozyme in 50 mM, pH 7.4 PBS (a), lysozyme extracted from fiber samples F1, F2 and F3 with protein loadings of 1.0% (A), 3.0% (B) and 5.0% (C) after incubation for 1 day (b), 1 week (c), 2 weeks (d), and free lysozyme after incubation with MC/PDLLA fibers for 2 weeks (e). (D) Specific bioactivity retention (S.A.R.) of native lysozyme (◆) and lysozyme extracted from the fiber samples F1 (■), F2 (●) and F3 (▲) during incubation ($n = 3$).

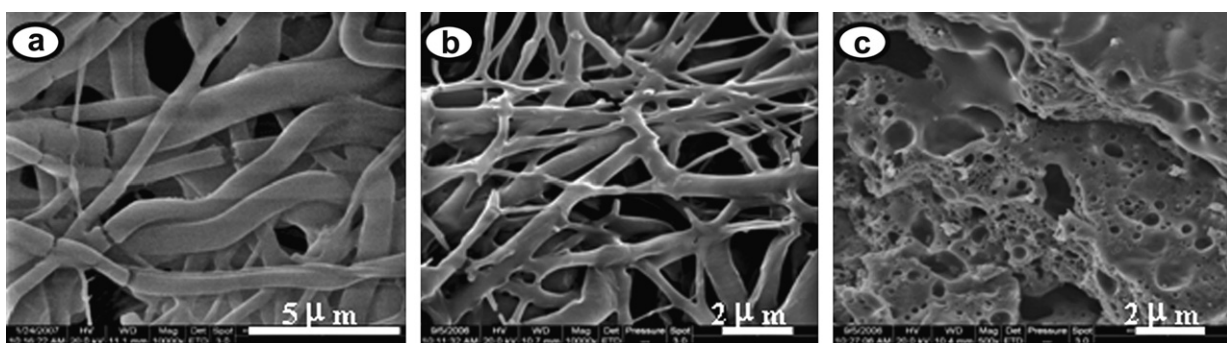


Fig. 6. SEM morphologies of lyz-MC/PDLLA fibers with lysozyme loading of 3.0% after incubated for 2 (a), 4 (b) and 8 (c) weeks in 50 mM pH 7.4 PBS at 37 °C.

Compared with the time zero data shown in Fig. 1, the fiber size increased after 2 weeks incubation, and the fiber space decreased and some fibers became collapsed due to chain relaxation of the matrix polymer after incubation into the medium with elevated temperature (Fig. 6a) [17]. After 4 weeks of incubation, most fibers shrank and collapsed from their previous cylindrical shape (Fig. 6b). This

may arise from the exhausted state of lyz/MC aggregates inside the polymer shell and the degradation of the polymer matrix. At week 8 after incubation, the lyz-MC/PDLLA fibers were fused into a porous film without distinct fiber structures (Fig. 6c).

Gravimetric evaluation of the mass loss of the electrospun fiber mat with and without protein loading is summa-

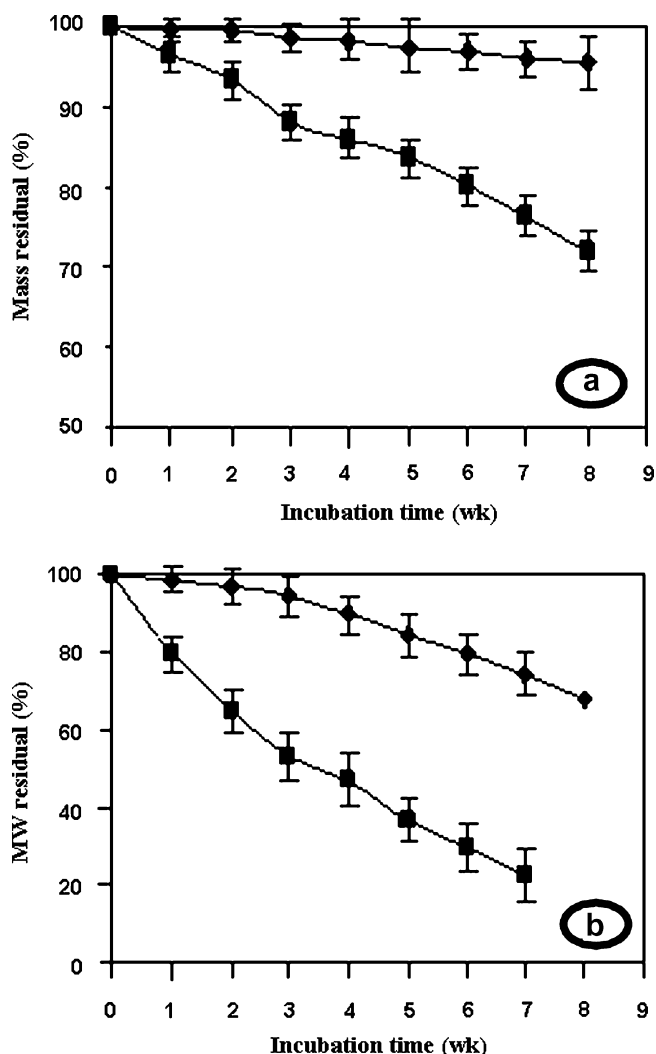


Fig. 7. *In vitro* degradation profiles. Mass loss (a) and molecular weight reduction (b) of lyz-MC/PDLLA fibrous mats (■) and MC/PDLLA fibrous mat without protein inoculation (◆) after incubated in 50 mM pH 7.4 PBS at 37 °C ($n = 3$).

ized in Fig. 7a. The mass loss of the fiber mat in the early stages may result from the protein, MC and other oligomers dissolving into the degradation medium, and this stage was short. In intermediate stages of degradation, the mass loss may be chiefly caused by the protein diffusing out of the fibers, which was confirmed based on the protein content and the reduced mass loss of the fibers without protein incorporation. More porous fibers formed after protein release out, and the high contacting area of matrix polymer with the degradation medium resulted in significant faster mass loss for fibers with than those without protein inoculation. Fig. 7b shows the molecular weight reduction of matrix polymer of fibers with and without protein loading as a function of incubation time. The molecular weight of the matrix polymer after 8 weeks of incubation could not be analyzed accurately for lyz-MC/PDLLA fibers. It shows that the rate of molecular weight loss for the lyz-MC/PDLLA fibers was much faster than

that of MC/PDLLA fiber mat without protein incorporation. With the protein release from lyz-MC/PDLLA fibers led to much more pores in the fibers, resulting in faster distribution of water into the fiber matrix and faster hydrolysis of polymer backbone.

4. Conclusions

Emulsion electrospinning was successfully introduced to prepare core-shell-structured ultrafine fibers, which could pronouncedly alleviate the initial burst release, prolong the release period dependent on the protein loading amount, and protect the structural integrity and bioactivity of encapsulated lysozyme during incubation in medium. The protein entrapment led to more significant mass loss and higher molecular weight reduction of the matrix residues. Current results provide a basis for further exploration of the structural stability and bioactivity of the encapsulated protein, in order to achieve highly sustainable, controllable, and effective protein-releasing kinetics of bioactive proteins, which would find better applications of electrospun fibers as tissue engineering scaffolds.

Acknowledgements

This work was supported by National Natural Science Foundation of China (30570501), Program for New Century Excellent Talents in University (NECT-06-0801), Specialized Research Fund for the Doctoral Program of Higher Education (20050613025), Ying Tong Education Foundation (104032), Ministry of Education of China.

References

- [1] L.A. Smith, P.X. Ma, Nano-fibrous scaffolds for tissue engineering, *Colloid Surf. B* 39 (2004) 125–131.
- [2] L. Cheng, S.M. Zhang, P.P. Chen, S.L. Huang, L. Liu, W. Zhou, J. Liu, H. Gong, Q.M. Luo, Fabrication and characterization of fluorohydroxyapatite nanocrystals/poly(D,L-lactide) composite scaffolds, *Curr. Appl. Phys.* 7 (2007) e71–e74.
- [3] R. Murugan, S. Rammakrishna, Nano-featured scaffolds for tissue engineering: a review of spinning methodologies, *Tissue Eng.* 12 (2006) 435–447.
- [4] W.J. Li, C.T. Laurencin, E.J. Caterson, R.S. Tuan, F.K. Ko, Electrospun nanofibrous structure: a novel scaffold for tissue engineering, *J. Biomed. Mater. Res.* 60 (2002) 613–621.
- [5] M. Goldberg, R. Langer, X. Jia, Nanostructured materials for applications in drug delivery and tissue engineering, *J. Biomat. Sci. Polym. Ed.* 18 (2007) 241–268.
- [6] K. Kim, Y.K. Luu, C. Chang, D. Fang, B.S. Hsiao, M. Hadjiargyrou, Incorporation and controlled release of a hydrophilic antibiotic using poly(lactide-co-glycolide)-based electrospun nanofibrous scaffolds, *J. Control. Release* 98 (2004) 47–56.
- [7] C.L. Casper, N. Yamaguchi, K.L. Kiick, J.F. Rabolt, Functionalizing electrospun fibers with biologically relevant macromolecules, *Biomacromolecules* 6 (2005) 1998–2007.
- [8] J. Zeng, A. Aigner, F. Czubayko, T. Kissel, J.H. Wendorff, A. Greiner, Poly(vinyl alcohol) nanofibers by electrospinning as a protein delivery system and the retardation of enzyme release by additional polymer coatings, *Biomacromolecules* 6 (2005) 1484–1488.

- [9] C. Li, C. Vepari, H.J. Jin, H.J. Kim, D.L. Kaplan, Electrospun silk-BMP-2 scaffolds for bone tissue engineering, *Biomaterials* 27 (2006) 3115–3124.
- [10] T.G. Kim, D.S. Lee, T.G. Park, Controlled protein release from electrospun biodegradable fiber mesh composed of poly(ϵ -caprolactone) and poly(ethylene oxide), *Int. J. Pharm.* 338 (2007) 276–283.
- [11] H. Qi, P. Hu, J. Xu, A. Wang, Encapsulation of drug reservoirs in fibers by emulsion electrospinning: morphology characterization and preliminary release assessment, *Biomacromolecules* 7 (2006) 2327–2330.
- [12] Y.Z. Zhang, X. Wang, Y. Feng, J. Li, C.T. Lim, S. Ramakrishna, Coaxial electrospinning of (fluorescein isothiocyanate-conjugated bovine serum albumin)-encapsulated poly(ϵ -caprolactone) nanofibers for sustained release, *Biomacromolecules* 7 (2006) 1049–1057.
- [13] H. Jiang, Y. Hu, P. Zhao, Modulation of protein release from biodegradable core-shell structured fibers prepared by coaxial electrospinning, *J. Biomed. Mater. Res.* 79A (2006) 50–57.
- [14] X. Xu, X. Zhuang, X. Chen, Preparation of core-sheath composite nanofibers by emulsion electrospinning, *Macromol. Rapid Commun.* 27 (2006) 1637–1642.
- [15] X. Xu, L. Yang, X. Chen, Ultrafine medicated fibers electrospun from W/O emulsions, *J. Control. Release* 108 (2005) 33–42.
- [16] X.M. Deng, M.L. Yuan, C.D. Xiong, X.H. Li, Polymerization of lactides and lactones. 2: Ring-opening polymerization of ϵ -caprolactone and dl-lactide by organoacid rare earth compounds, *J. Appl. Polym. Sci.* 71 (1999) 1941–1948.
- [17] W.G. Cui, X.H. Li, X.L. Zhu, G. Yu, S.B. Zhou, J. Weng, Investigation of drug release and matrix degradation of electrospun poly(DL-lactide) fibers with paracetamol inoculation, *Biomacromolecules* 7 (2006) 1623–1629.
- [18] M.M. Bradford, A rapid and sensitive method for the quantitation of microgram quantities of protein utilizing the principle of protein-dye binding, *Anal. Biochem.* 72 (1976) 248–254.
- [19] H. Rafati, A.G.A. Coombes, J. Adler, J. Holland, S.S. Davis, Protein-loaded poly(DL-lactide-co-glycolide) microparticles for oral administration: formulation, structural and release characteristics, *J. Control. Release* 43 (1997) 89–102.
- [20] H. Susi, D.M. Byler, Protein structure by Fourier transform infrared spectroscopy: second derivative spectra, *Biochem. Biophys. Res.* 115 (1983) 391–397.
- [21] C. Perez, P.D. Jesus, K. Griebenow, Preservation of lysozyme structure and function upon encapsulation and release from poly(lactic-co-glycolic) acid microspheres prepared by the water-in-oil-in-water method, *Int. J. Pharm.* 248 (2002) 193–206.
- [22] K. Fu, K. Griebenow, L. Hsieh, FTIR characterization of the secondary structure of proteins encapsulated within PLGA microspheres, *J. Control. Release* 58 (1999) 357–366.
- [23] F.T. Meng, G.H. Ma, W. Qiu, Z.G. Su, W/O/W double emulsion technique using ethyl acetate as organic solvent: effects of its diffusion rate on the characteristics of microparticles, *J. Control. Release* 91 (2003) 407–416.
- [24] J.H. Yu, S.V. Fridrikh, G.C. Rutledge, Production of submicrometer diameter fibers by two-fluid electrospinning, *Adv. Mater.* 16 (2004) 1562–1566.
- [25] P.I. Haris, D. Chapman, Does Fourier-transform infrared spectroscopy provide useful information on protein structures? *Trends Biochem. Sci.* 17 (1992) 328–333.
- [26] A. Poetsch, S. Rexroth, J. Heberle, T.A. Link, N.A. Dencher, H. Seelert, Characterisation of subunit III and its oligomer from spinach chloroplast ATP synthase, *Biochim. Biophys. Acta* 1618 (2003) 59–66.
- [27] I.H. Parvez, S. Feride, FTIR spectroscopic characterization of protein structure in aqueous and non-aqueous media, *J. Mol. Catal. B Enzym.* 7 (1999) 207–221.
- [28] M. Jonathan Hadden, D. Chapman, D.C. Lee, A comparison of infrared spectra of proteins in solution and crystalline forms, *Biochim. Biophys. Acta* 1248 (1995) 115–122.
- [29] D.M. Byler, H. Susi, Examination of the secondary structure of proteins by deconvolved FTIR spectra, *Biopolymers* 25 (1986) 469–487.
- [30] E. Querol, J.A. Perez-Pons, A. Mozo-Villarias, Analysis of protein conformational characteristics related to thermostability, *Protein Eng.* 9 (1996) 265–271.
- [31] S.B. Zhou, X.M. Deng, X.H. Li, Investigation on a novel core-coated microspheres protein delivery system, *J. Control. Release* 75 (2001) 27–36.